Draft version June 22, 2023
Typeset using LaTeX **twocolumn** style in AASTeX631

Early Structure Formation from Primordial Density Fluctuations with a Blue, Tilted Power Spectrum - II. High-Redshift Galaxies

Shingo Hirano [1] and Naoki Yoshida [2,3,4]

[1] *Department of Astronomy, School of Science, The University of Tokyo, 7-3-1 Hongo, Bunkyo, Tokyo 113-0033, Japan*
[2] *Department of Physics, School of Science, The University of Tokyo, 7-3-1 Hongo, Bunkyo, Tokyo 113-0033, Japan*
[3] *Research Center for the Early Universe, School of Science, The University of Tokyo, 7-3-1 Hongo, Bunkyo, Tokyo 113-0033, Japan*
[4] *Kavli Institute for the Physics and Mathematics of the Universe (WPI), UT Institutes for Advanced Study, The University of Tokyo, Kashiwa, Chiba 277-8583, Japan*

ABSTRACT

The first series of observations by the James Webb Space Telescope (JWST) discovered unexpectedly abundant luminous galaxies at high redshift, posing possibly a serious challenge to popular galaxy formation models. We study early structure formation in a cosmological model with a blue, tilted power spectrum (BTPS) given by $P(k) \propto k^{m_{\rm s}}$ with $m_{\rm s} > 1$ at small length scales. We run a set of cosmological N-body simulations and derive the abundance of dark matter halos and of galaxies under simplified assumptions on star formation efficiency. The enhanced small-scale power allows rapid formation of nonlinear structure at $z > 7$, and galaxies with stellar mass exceeding $10^{10}\,M_\odot$ can be formed by $z = 9$. Because of frequent mergers, the structure of galaxies and galaxy groups appears overall clumpy. The BTPS model reproduces the observed stellar mass density at $z = 7 - 9$, and thus eases the claimed tension between galaxy formation theory and recent JWST observations. Large-scale structure of the present-day Universe is largely unaffected by the modification of the small-scale power spectrum. Finally, we discuss the formation of the first stars and early super-massive black holes in the BTPS model.

Keywords: Cosmology (343) — Dark matter (353) — Early universe (435) — Galaxy formation (595) — Population III stars (1285)

1. INTRODUCTION

The so-called Λ Cold Dark Matter (ΛCDM) cosmology successfully reproduces a broad range of observations of the large-scale structure of the Universe, and thus has been established as the standard cosmological model. An important element of the standard model is the primordial density fluctuations generated in the very early universe with a nearly scale-independent power spectrum. While the large-scale density fluctuations have been observationally probed to $k \sim 1\,{\rm Mpc}^{-1}$, the amplitude and the shape of the power spectrum on smaller, (sub-)galactic length scales are poorly constrained (e.g., Hlozek et al. 2012; Bullock & Boylan-Kolchin 2017). Hence theoretical studies on galaxy formation often rely on significant extrapolation of the assumed scale-invariant primordial power spectrum (PPS).

Various possibilities have been proposed from the physics of the early universe that posit deviations from scale-invariance. Blue, tilted or enhanced power spectra can arise in beyond-standard cosmological models (e.g., Covi & Lyth 1999; Martin & Brandenberger 2001; Gong & Sasaki 2011; Inman & Kohri 2022), and yield a number of interesting cosmological and astrophysical consequences (e.g., Clesse & García-Bellido 2015; Germani & Prokopec 2017). Earlier in Hirano et al. (2015), we studied early structure formation in models with a blue, tilted power spectrum (BTPS). It was shown that the enhanced small-scale density fluctuations drive the formation of nonlinear structure and of the first stars at very early epochs.

In this *Letter*, we study the formation and abundance of the first galaxies in the BTPS model in light of re-

Corresponding author: Shingo Hirano
hirano@astron.s.u-tokyo.ac.jp

Table 1. List of three models

PPS model	$k_{\rm p}$	$m_{\rm s}$	σ_8	$L_{\rm box}$	$\{\epsilon_{\rm min}, \epsilon_{\rm mean}, \epsilon_{\rm max}\}$	$\{\epsilon_{\rm min}, \epsilon_{\rm mean}, \epsilon_{\rm max}\}$
	$(h\,{\rm cMpc}^{-1})$			$({\rm cMpc}\,h^{-1})$	at $z = 9$	at $z = 7.5$
(1)	(2)	(3)	(4)	(5)	(6)	(7)
Hard-tilt	1.0	2.0	0.8114093	10, 25, 50	{0.07, 0.12, 0.24}	{0.13, 0.30, 0.70}
Soft-tilt	1.0	1.5	0.8112334	10, 25, 50	{0.10, 0.18, 0.32}	{0.17, 0.40, 0.97}
ΛCDM	-	-	0.8111	10, 25, 50	{0.17, 0.35, 0.64}	{0.25, 0.60, 1.46}

NOTE— Column (1): model name. Column (2): pivot scale ($k_{\rm p}$). Column (3): tilt index ($m_{\rm s}$). Column (4): root-mean-square matter fluctuation averaged over a sphere of radius $8\,h^{-1}\,{\rm Mpc}$ (σ_8). Column (5): periodic box length ($L_{\rm box}$). Columns (6) and (7): star formation efficiencies required to exceed the lower limit, center, and upper limit of the observation-limited CCSMD region ($\epsilon_{\rm min}$, $\epsilon_{\rm mean}$, $\epsilon_{\rm max}$) at $z = 9$ and 7.5.

cent observations by the James Webb Space Telescope (JWST). A number of galaxies (candidates) with unexpectedly high stellar masses have been discovered (e.g., Finkelstein et al. 2022; Labbé et al. 2023). Boylan-Kolchin (2023) concludes that the inferred high stellar masses of the observed galaxy candidates require an extremely high star formation efficiency far exceeding plausible values of $\epsilon \lesssim 0.3$ suggested by popular galaxy formation models (Gribel et al. 2017; Tacchella et al. 2018; Behroozi et al. 2020). The challenge brought by recent JWST observations motivates us to reconsider either the detailed physics of galaxy formation in the early universe or the standard cosmology model.

Modification of PPS may provide a viable solution by promoting early structure formation (Parashari & Laha 2023; Padmanabhan & Loeb 2023). Parashari & Laha (2023) compute the cumulative comoving stellar mass density (CCSMD) by adopting a modified form of PPS similar to Hirano et al. (2015). Their model can successfully reproduce the observed CCSMD *without* assuming an unrealistically high star formation efficiency. They further argue that observations of high-redshift galaxies can provide invaluable information on small-scale density fluctuations that otherwise cannot be probed directly. Clearly, it is important and timely to study the formation of high-redshift galaxies by performing cosmological simulations for the BTPS model.

Throughout the present *Letter*, we adopt the cosmological parameters with total matter density $\Omega_{\rm m} = 0.3153$, baryon density $\Omega_{\rm b} = 0.0493$ in units of the critical density, a Hubble constant $H_0 = 67.36\,{\rm km\,s^{-1}\,Mpc^{-1}}$, the root-mean-square matter fluctuation averaged over a sphere of radius $8\,h^{-1}\,{\rm Mpc}$ $\sigma_8 = 0.8111$, and primordial index $n_{\rm s} = 0.9649$ (Planck Collaboration et al. 2020).

2. NUMERICAL SIMULATIONS

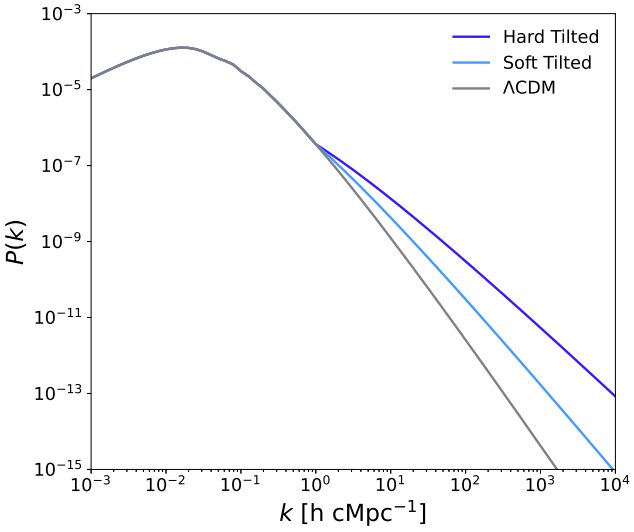

Figure 1. The matter power spectra at $z = 1089$ that we use to generate the cosmological initial conditions. The gray line is for the standard ΛCDM model, whereas the other lines show the blue-tilted models with the pivot scale $k_{\rm p} = 1\,h\,{\rm cMpc}^{-1}$ and the tilt $m_{\rm s} = 1.5$ (soft-tilt) and 2.0 (hard-tilt), respectively.

We largely follow the method of our previous study (Hirano et al. 2015) to perform cosmological N-body simulations for models with three different PPS.

2.1. *Primordial power spectrum*

The standard, scale-independent PPS is given by

$$P_{\rm prim}(k) \propto k^{n_{\rm s}}\,, \tag{1}$$

whereas the one with enhancement at small scales is given by

$$P_{\rm prim}(k) \propto k^{n_{\rm s}}\ ({\rm for}\ k \le k_{\rm p})\,, \tag{2}$$

$$\propto k_{\rm p}^{n_{\rm s}-m_{\rm s}} \cdot k^{m_{\rm s}}\ ({\rm for}\ k > k_{\rm p})\,. \tag{3}$$

We fix the pivot scale $k_{\rm p} = 1\,h\,{\rm cMpc}^{-1}$ (h comoving ${\rm Mpc}^{-1}$) and adopt two values $m_{\rm s} = 1.5$ and 2.0, which

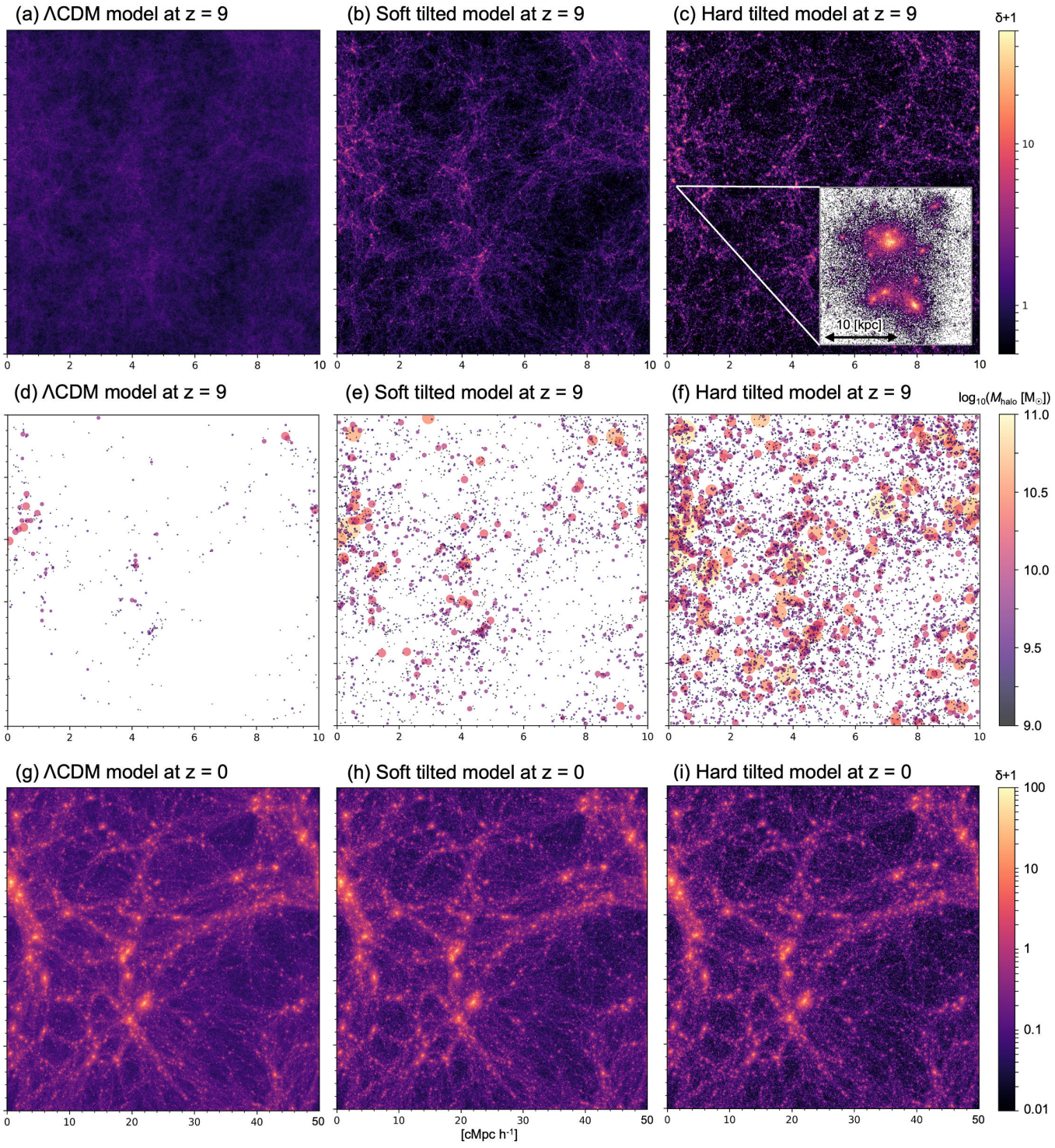

Figure 2. Projected density distributions $\delta + 1 = \rho/\bar{\rho}$ and DM halos with $M_{\rm halo} \geq 10^9\,M_\odot$. The top and middle panels show the structure at $z = 9$ in a volume of side-length $10\,{\rm cMpc}\,h^{-1}$, whereas the bottom panels show large-scale structure at $z = 0$ with a side-length of $50\,{\rm cMpc}\,h^{-1}$. The left, center, and right panels are for ΛCDM, soft-tilt, and hard-tilt models. The circle size in the middle panels scales with the halo mass. The inset in panel (c) is a zoom-in image of one of the most massive halos.

we call "soft-tilt" and "hard-tilt", respectively. We note that our soft-tilt model is in marginally acceptable parameter space from available observational constraints (see Figure 2 in Parashari & Laha 2023).

For the BTPS models, we adjust the normalization σ_8 to ensure that the amplitude of the fluctuations at large wavelength above the pivot scale is the same as in the standard ΛCDM model. Figure 1 shows the resulting matter power spectra at $z = 1089$.

2.2. *Cosmological simulations*

We use the public code `MUSIC` (Hahn & Abel 2011) to generate cosmological initial conditions. We employ 512^3 dark matter particles in comoving cubes of $L_{\rm box} = 10$, 25, and $50\,{\rm cMpc}\,h^{-1}$.Three different simulation volumes are adopted to derive the statistics of nonlinear structure accurately over a wide range of length and mass scales. The particle mass is 6.52×10^5, 1.02×10^7, and $8.15 \times 10^7\,M_\odot$, respectively. Dark matter halos with $M_{\rm halo} = 10^8\,M_\odot$ are resolved by more than 150 particles in our highest-resolution runs. Table 1 summarizes the basic simulation parameters. We use the parallel N-body code `GADGET-2` (Springel 2005) to follow structure formation from redshift $z = 99$ to 0.

2.3. *Analysis*

We follow Boylan-Kolchin (2023) and Parashari & Laha (2023) to compute the cumulative comoving stellar mass density (CCSMD) from the simulation outputs. We determine the required star formation efficiency (ϵ) to reconcile the recent JWST observation.

We first run a Friends-of-Friends group finder with linking length $b = 0.164(m/\bar{\rho}(z))^{-3}$, where m is the N-body particle mass and $\bar{\rho}(z)$ is the mean density of the universe at redshift z, to obtain the halo mass function ${\rm d}n(M,z)/{\rm d}M$. We combine the halo mass functions from our simulations with different volumes (particle masses) to construct the halo mass function for each model in a wide mass range. Next, we calculate the cumulative comoving mass density of halos

$$\rho(\geq M_{\rm halo}, z) = \int_{M_{\rm halo}}^{\infty} {\rm d}M M \frac{{\rm d}n(M,z)}{{\rm d}M}\,. \qquad (4)$$

Finally, we compute the CCSMD with stellar mass larger than M_* at each redshift, $\rho_*(\geq M_*, z) = \epsilon f_{\rm b}\rho(\geq M_{\rm halo}, z)$. We assume $M_* = \epsilon f_{\rm b} M_{\rm halo}$, where $f_{\rm b} = \Omega_{\rm b}/\Omega_{\rm m}$, and also assume that the star formation efficiency $\epsilon(\leq 1)$ is constant over the redshift range we consider.

3. RESULTS

Figure 2 shows the projected density distributions for the three models. The enhanced small-scale density fluctuations yield stronger density contrast in the BTPS models than in the ΛCDM model; numerous nonlinear objects (halos) are already formed by $z = 9$. We compare the halo mass functions in Figure 3, which will be used later to discuss the cumulative stellar mass. The number density of halos with mass $10^9 < M/M_\odot < 10^{11}$ differs by an order of magnitude between the hard-tilt model and the ΛCDM model.

The middle panels of Figure 2 show that massive galaxies (halos) are strongly clustered in the BTPS models. The relative galaxy bias with respect to the underlying dark matter distribution will provide crucial information on the nature of the early galaxy population. Future wide-field observations of galaxy distribution and clustering by JWST or the Roman Space Telescope will enable us to discriminate theoretical models of galaxy formation (Muñoz et al. 2023).

The bottom panels of Figure 2 suggest that the large-scale structure of several tens Mpc in the present-day universe ($z = 0$) remains essentially the same. Clearly, the enhancement of PPS at the small length scales does not ruin the success of the ΛCDM model. The same holds for the halo mass function at $z = 0$ plotted in Figure 3(c).

Figure 4 shows the CCSMDs for the three models at $z = 9$ and 7.5. There we assume $\epsilon = 0.1$ (solid lines) and 0.3 (dashed lines) with the latter corresponding to the plausible upper limit suggested by theoretical models of galaxy formation (Gribel et al. 2017; Tacchella et al. 2018; Behroozi et al. 2020). The green regions indicate the JWST observations adopted from Parashari & Laha (2023), who calculated the CCSMD from the observation of Labbé et al. (2023) with the corresponding spectroscopic updates in two redshift bins $z \in [7, 8.5]$ and $[8.5, 10]$ using the three most massive galaxies.

As has been suggested in the recent literature, a large value of $\epsilon \sim 0.3$ is required for the ΛCDM model to reproduce the mean value of the observed CCSMD at $z = 9$ (Figure 4a). Even with the "maximal" ϵ, the CCSMD does not reach the lower limit of the uncertainty range of the observations at $z = 7.5$ (Figure 4b). The CCSMD of the soft-tilt model is about ten and three times larger than the ΛCDM model at $z = 9$ and 7.5, respectively. Thus the soft-tilt model requires a moderate star formation efficiency of $\epsilon \sim 0.1 - 0.3$ to match the observed CCSMDs both at $z = 9$ and 7.5. Table 1 summarizes the star formation efficiency required for the CCSMD of each model to exceed the observationally inferred lower limit ($\epsilon_{\rm min}$), mean ($\epsilon_{\rm mean}$), and upper limit ($\epsilon_{\rm max}$).

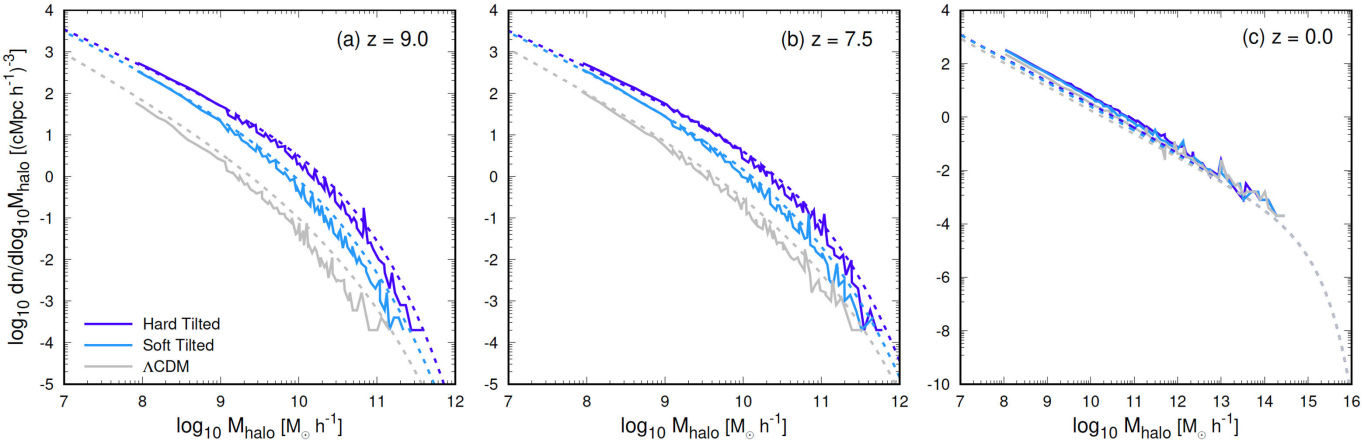

Figure 3. Halo mass functions at $z = 9$, 7.5, and 0 from left to right. The solid lines show our simulation results and the dashed lines represent the analytical Sheth–Tormen mass functions (Sheth & Tormen 1999) calculated by the public code `genmf` (Reed et al. 2007). The gray, light blue, and dark blue lines are for the ΛCDM, soft-tilted, and hard-tilted models. We construct the simulation data by combining results for different box sizes, $L_{\rm box} = 10$, 25, and 50 cMpc h^{-1}.

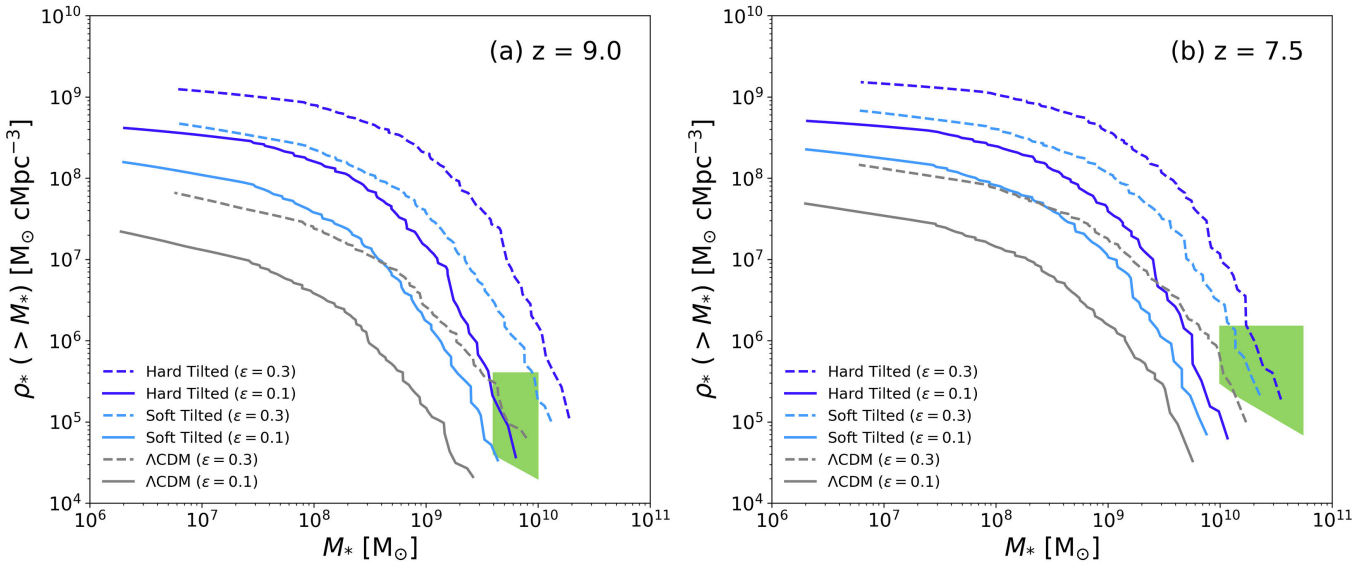

Figure 4. Cumulative comoving stellar mass density (CCSMD) for the ΛCDM (gray), soft-tilted (light blue), and hard-tilted (blue) models at $z = 9$ (panel a) and 7.5 (b). We adopt moderate star formation efficiency of $\epsilon = 0.1$ (solid lines) and 0.3 (dashed lines). The green regions are the CCSMD adopted from Parashari & Laha (2023) for the observations of Labbé et al. (2023).

4. DISCUSSION

The result of our cosmological simulations is largely consistent with the estimate of Parashari & Laha (2023) based on analytic halo mass functions. Our simulations confirm that the standard ΛCDM model requires unrealistically high star formation efficiencies of $\epsilon > 0.3$ to reconcile the observed CCSMD. Although there have already been proposals for galaxy formation physics that can realize a high star formation efficiency (e.g., Dekel et al. 2023), a slight modification of the PPS may be another promising solution that alleviates the need for large deviation from the currently popular galaxy formation models.

Interestingly, recent JWST observations also show that there are many galaxies with clumpy structures and also galaxies in the process of mergers in proto-cluster environments at $z = 7-9$ (Hashimoto et al. 2023; Hainline et al. 2023). Nonlinear structure forms early in the BTPS model, assembles via mergers, and thus galaxies at $z = 7-9$ tend to appear clumpy, as seen in Figure 2.

The formation epoch and the properties of the first stars are strongly affected by the PPS. Hirano et al. (2015) run a set of hydrodynamics simulations starting from nearly the same BTPS, and find that very massive stars with mass exceeding $100\,M_\odot$ are formed early. Xing et al. (2023) discovered a metal-poor star that shows definite chemical signatures of the so-called pair-instability supernova caused by a very massive star early in the formation history of the Milky Way.

The existence of super-massive black holes in the early universe generally suggests rapid growth of structure and formation of appropriate seed black holes at early epochs (e.g., Inayoshi et al. 2020). Larson et al. (2023) discovered a massive black hole candidate at $z = 8.6$. Stellar-mass black holes are formed as remnants of massive Population III stars as early as $z \sim 50 - 100$ in the BTPS model, leaving enough time for the seeds to grow by mass accretion to massive black holes by $z = 8$. Frequent halo mergers realized in the BTPS model may also enhance the formation of massive black holes in the early universe (Wise et al. 2019; Regan 2023).

Tight constraints can be placed on the slope or the amplitude of PPS at sub-galactic length scales from the epoch of reionization. Contribution to reionization from individual Population III stars is severely limited by the measurement of the Thomson optical depth by Planck (Visbal et al. 2015). Since there still remains substantial uncertainty in both observations of reionization history (Hinshaw et al. 2013; Planck Collaboration et al. 2020; Forconi et al. 2023) and in astrophysical modeling (Fialkov 2022), it would be necessary to perform detailed numerical simulations of galaxy formation and reionization for the BTPS model.

JWST has opened a new window into the distant universe. Future observations by JWST and by other cosmology surveys will reveal the physical properties and the formation history of galaxy *populations* at high redshift, and will ultimately provide new insight into the early universe physics that generates the primordial density fluctuations from which the first galaxies are formed.

Numerical computations were carried out on Cray XC50 at CfCA in National Astronomical Observatory of Japan and Yukawa-21 at YITP in Kyoto University. Numerical analyses were in part carried out on the analysis servers at CfCA in National Astronomical Observatory of Japan. This work was supported by JSPS KAKENHI Grant Numbers JP21K13960, JP21H01123, and JP22H01259 (S.H.), and MEXT as "Program for Promoting Researches on the Supercomputer Fugaku" (Structure and Evolution of the Universe Unraveled by Fusion of Simulation and AI; Grant Number JPMXP1020230406, Project ID hp230204) (S.H. and N.Y).

REFERENCES

Behroozi, P., Conroy, C., Wechsler, R. H., et al. 2020, MNRAS, 499, 5702, doi: 10.1093/mnras/staa3164

Boylan-Kolchin, M. 2023, Nature Astronomy, doi: 10.1038/s41550-023-01937-7

Bullock, J. S., & Boylan-Kolchin, M. 2017, ARA&A, 55, 343, doi: 10.1146/annurev-astro-091916-055313

Clesse, S., & García-Bellido, J. 2015, PhRvD, 92, 023524, doi: 10.1103/PhysRevD.92.023524

Covi, L., & Lyth, D. H. 1999, PhRvD, 59, 063515, doi: 10.1103/PhysRevD.59.063515

Dekel, A., Sarkar, K. C., Birnboim, Y., Mandelker, N., & Li, Z. 2023, MNRAS, 523, 3201, doi: 10.1093/mnras/stad1557

Fialkov, A. 2022, in The Fifteenth Marcel Grossmann Meeting on General Relativity. Edited by E. S. Battistelli, ed. E. S. Battistelli, R. T. Jantzen, & R. Ruffini, 1067–1073, doi: 10.1142/9789811258251_0149

Finkelstein, S. L., Bagley, M. B., Haro, P. A., et al. 2022, ApJL, 940, L55, doi: 10.3847/2041-8213/ac966e

Forconi, M., Ruchika, Melchiorri, A., Mena, O., & Menci, N. 2023, arXiv e-prints, arXiv:2306.07781, doi: 10.48550/arXiv.2306.07781

Germani, C., & Prokopec, T. 2017, Physics of the Dark Universe, 18, 6, doi: 10.1016/j.dark.2017.09.001

Gong, J.-O., & Sasaki, M. 2011, JCAP, 2011, 028, doi: 10.1088/1475-7516/2011/03/028

Gribel, C., Miranda, O. D., & Williams Vilas-Boas, J. 2017, ApJ, 849, 108, doi: 10.3847/1538-4357/aa921a

Hahn, O., & Abel, T. 2011, MNRAS, 415, 2101, doi: 10.1111/j.1365-2966.2011.18820.x

Hainline, K. N., Johnson, B. D., Robertson, B., et al. 2023, arXiv e-prints, arXiv:2306.02468, doi: 10.48550/arXiv.2306.02468

Hashimoto, T., Álvarez-Márquez, J., Fudamoto, Y., et al. 2023, arXiv e-prints, arXiv:2305.04741, doi: 10.48550/arXiv.2305.04741

Hinshaw, G., Larson, D., Komatsu, E., et al. 2013, ApJS, 208, 19, doi: 10.1088/0067-0049/208/2/19

Hirano, S., Zhu, N., Yoshida, N., Spergel, D., & Yorke, H. W. 2015, ApJ, 814, 18, doi: 10.1088/0004-637X/814/1/18

Hlozek, R., Dunkley, J., Addison, G., et al. 2012, ApJ, 749, 90, doi: 10.1088/0004-637X/749/1/90

Inayoshi, K., Visbal, E., & Haiman, Z. 2020, ARA&A, 58, 27, doi: 10.1146/annurev-astro-120419-014455

Inman, D., & Kohri, K. 2022, arXiv e-prints, arXiv:2207.14735, doi: 10.48550/arXiv.2207.14735

Labbé, I., van Dokkum, P., Nelson, E., et al. 2023, Nature, 616, 266, doi: 10.1038/s41586-023-05786-2

Larson, R. L., Finkelstein, S. L., Kocevski, D. D., et al. 2023, arXiv e-prints, arXiv:2303.08918, doi: 10.48550/arXiv.2303.08918

Martin, J., & Brandenberger, R. H. 2001, PhRvD, 63, 123501, doi: 10.1103/PhysRevD.63.123501

Muñoz, J. B., Mirocha, J., Furlanetto, S., & Sabti, N. 2023, arXiv e-prints, arXiv:2306.09403, doi: 10.48550/arXiv.2306.09403

Padmanabhan, H., & Loeb, A. 2023, arXiv e-prints, arXiv:2306.04684, doi: 10.48550/arXiv.2306.04684

Parashari, P., & Laha, R. 2023, arXiv e-prints, arXiv:2305.00999, doi: 10.48550/arXiv.2305.00999

Planck Collaboration, Aghanim, N., Akrami, Y., et al. 2020, A&A, 641, A6, doi: 10.1051/0004-6361/201833910

Reed, D. S., Bower, R., Frenk, C. S., Jenkins, A., & Theuns, T. 2007, MNRAS, 374, 2, doi: 10.1111/j.1365-2966.2006.11204.x

Regan, J. 2023, The Open Journal of Astrophysics, 6, 12, doi: 10.21105/astro.2210.04899

Sheth, R. K., & Tormen, G. 1999, MNRAS, 308, 119, doi: 10.1046/j.1365-8711.1999.02692.x

Springel, V. 2005, MNRAS, 364, 1105, doi: 10.1111/j.1365-2966.2005.09655.x

Tacchella, S., Bose, S., Conroy, C., Eisenstein, D. J., & Johnson, B. D. 2018, ApJ, 868, 92, doi: 10.3847/1538-4357/aae8e0

Visbal, E., Haiman, Z., & Bryan, G. L. 2015, MNRAS, 453, 4456, doi: 10.1093/mnras/stv1941

Wise, J. H., Regan, J. A., O'Shea, B. W., et al. 2019, Nature, 566, 85, doi: 10.1038/s41586-019-0873-4

Xing, Q.-F., Zhao, G., Liu, Z.-W., et al. 2023, Nature, , doi: 10.1038/s41586-023-06028-1